Geophysical Research Letters

RESEARCH LETTER
10.1029/2019GL082714

The Role of the Tropically Excited Arctic Warming Mechanism on the Warm Arctic Cold Continent Surface Air Temperature Trend Pattern

Joseph P. Clark[1] **and Sukyoung Lee**[1]

[1]Department of Meteorology and Atmospheric Science, The Pennsylvania State University, University Park, PA, USA

Key Points:
- The wintertime warm Arctic cold continent surface air temperature trend pattern was preceded by a period with the reverse trend pattern
- The circulation is driving the observed warm Arctic cold continent surface air temperature trend pattern
- La Niña-like tropical convection contributed to the warm Arctic cold continent surface air temperature trend pattern

Supporting Information:
- Supporting Information S1

Correspondence to:
J. P. Clark,
juc414@psu.edu

Citation:
Clark, J. P., & Lee, S. (2019). The role of the Tropically Excited Arctic Warming Mechanism on the warm Arctic cold continent surface air temperature trend pattern. *Geophysical Research Letters*, *46*, 8490–8499. https://doi.org/10.1029/2019GL082714

Received 10 MAR 2019
Accepted 6 JUN 2019
Accepted article online 1 JUL 2019
Published online 29 JUL 2019

Abstract The December–February surface air temperature (SAT) trend is examined for all consecutive 20-year time periods between 1979 and 2017, from which a transition from a cold-Arctic-warm-continent toward a warm-Arctic-cold-continent trend pattern is evident. This transition is accompanied by a consistent transition in the sea level pressure trend pattern that supports warm air advection over the Arctic and cold air advection over the continents. The regression of the detrended December–February-average SAT onto a detrended index defined to quantify the east-west gradient of tropical Pacific sea surface temperature is characterized by a warm-Arctic-cold-continent pattern much like the SAT trend pattern observed in recent decades. A decadal timescale warming of the western tropical Pacific water has increased the east-west gradient of tropical Pacific sea surface temperature, thus contributing to the observed extratropical SAT trend transition.

Plain Language Summary Over the last two decades, Arctic surface temperatures have been increasing rapidly—at a rate faster than anywhere else on the globe. Concurrent with this rapid increase of Arctic surface temperatures, surface temperatures over the North American and Eurasian continents have decreased. This simultaneous warming of the Arctic and cooling of the continents was preceded by a period of simultaneous Arctic cooling and continental warming.
The transition from the period of Arctic cooling and continental warming toward the present period of Arctic warming and continental cooling was likely caused by southerly winds (flowing from south to north) over the Arctic and northerly winds (flowing from north to south) over the continents. These winds move warm air into the Arctic and cold air over the continents. We present evidence that these circulation changes, and the associated temperature changes, are driven in part by the warming of the western tropical Pacific water (relative to the eastern tropical Pacific), which started at about the same time that the above transition occurred. The chain of events that link warming of the western equatorial tropical Pacific Ocean to circulation changes over the Arctic and continents is discussed in previous studies.

1. Introduction

Over the last several decades, the Arctic is warming faster than anywhere else, at about twice the rate of the global average (e.g., Chylek et al., 2009)—a phenomenon termed Arctic amplification. However, over the same time period that the Arctic has warmed, the continents have cooled (Cohen et al., 2012, 2014; Sun et al., 2016), prompting studies into the question of whether continental cold extremes can be caused by Arctic amplification (Francis & Vavrus, 2012) or sea ice decline (e.g., Nakamura et al., 2016; Sun et al., 2015; Zhang et al., 2018)

The hypothesized causal link between sea ice decline and continental cooling (e.g., Nakamura et al., 2016; Sun et al., 2015; Zhang et al., 2018) follows the viewpoint that summertime sea ice loss, which is amplified by the sea ice albedo feedback mechanism (Budyko, 1969; Sellers, 1969), causes upward surface heat fluxes during the subsequent winter, when the temperature difference between the newly exposed sea surface and overlying air is greatest (Deser et al., 2010). From this perspective, the surface heat fluxes associated with sea ice loss cause both near-surface temperature increases and excite Rossby waves that can propagate upward and decelerate the stratospheric polar vortex (e.g., Nakamura et al., 2016; Sun et al., 2015; Zhang et al., 2018). The tropospheric circulation changes that follow the decelerated stratospheric polar vortex favor cold advection over the continents (e.g., Nakamura et al., 2016), akin to the negative phase of the northern annular

mode (e.g., Thompson & Wallace, 2000), supporting the idea that sea ice decline causes both Arctic amplification and continental cooling.

In contrast to the hypothesis that sea ice decline causes both Arctic amplification and continental cooling, with observational data, Sorokina et al. (2016) showed that cold air outbreaks over Siberia coincide with downward, rather than upward, surface heat fluxes over the Barents and Kara Seas. An examination of the temperature response to historical forcing in several atmospheric general circulation and fully coupled climate models also supports the possibility that the continental cooling trend is not driven by sea ice loss (Sun et al., 2016). Instead, the fact that the multimodel mean temperature response to the historical radiative forcing is characterized by warming everywhere with a weak midlatitude circulation response is taken as evidence for internal variability being the ultimate cause of the recent continental cooling trend (Sun et al., 2016). Furthermore, that the Pacific Decadal Oscillation (PDO) has been predominately negative in recent decades is also often taken as evidence to support the viewpoint that internal variability is driving a large fraction of continental cooling trend (Screen & Francis, 2016; Trenberth et al., 2014). While Screen and Francis (2016) argue that the PDO has changed the climate response to sea ice loss, so as to enhance Arctic warming, Trenberth et al. (2014) argue that the negative PDO observed in recent decades has led to enhanced tropical convection over the central tropical Pacific. Ding et al. (2014) concluded that during 1979-2012, tropical Pacific SST trends contributed about half of the warming over northeastern Canada and Greenland. As in Sun et al. (2016), based on the fact that the climate model average that they examined did not capture the temperature trend, Ding et al. (2014) concluded that internal variability accounted for the warming.

While it is indeed common to assume that averages across model simulations represent the true response to climate forcing, recent studies show that the simulated mean climate during the historical period over the Arctic Ocean and continents is systematically biased (Woods et al., 2017) and the same bias pattern emerges in Representative Concentration Pathway 8.5 projections (Lee et al., 2019), diminishing the confidence that should be placed on the widespread assumption. As noted by Lee et al. (2019), systematic model bias can affect the multimodel mean projection, bringing to question the common practice of considering the deviation from the multimodel mean as internal variability. Moreover, the possibility that climate change embodies circulation changes as well as temperature changes implies that temperature changes caused by circulation changes should not be dismissed altogether as internal variability.

Along these lines, the Tropically Excited Arctic warming Mechanism [TEAM; Lee, 2012, 2014] suggests that the circulation is an important contributor to the temperature changes associated with climate change. Under this hypothesis, La Niña-like tropical convection, associated with a decadal timescale warming of the western tropical Pacific, triggers poleward propagating Rossby waves that constructively interfere with the climatological stationary wave (Goss et al., 2016) and subsequently flux warm and moist air into the Arctic. The observed bottom-heavy Arctic temperature trend, often cited as evidence for the sea ice albedo feedback mechanism (e.g., Screen & Simmonds, 2010), does not deviate from TEAM (Yoo et al., 2014): The climatological temperature inversion in the Arctic boundary layer is eroded by horizontal temperature advection (Baggett et al., 2016; Woods & Caballero, 2016), which may explain why the Arctic winter warming trend is strongest near the surface. Because constructive interference with the climatological stationary wave has been linked to vertically propagating Rossby waves that decelerate the stratospheric polar vortex (e.g., Garfinkel et al., 2010, 2012; Nishii et al., 2009), the TEAM may also plausibly account for the recent downward trend in continental surface air temperature (SAT). Consistently, Lee (2012) showed that La Niña is associated with warmer than average Arctic temperatures and colder than average continental temperatures.

In this study, we therefore address a question different from previous studies on the warm Arctic cold continent pattern, by asking whether or not the TEAM is contributing to the observed warm-Arctic-cold-continent SAT trend pattern. Specifically, we ask (1) whether extratropical SAT tends to take on the warm Arctic cold continent pattern when western tropical Pacific water is anomalously warmer than eastern tropical Pacific water, (2) whether there has been a decadal timescale warming of the western tropical Pacific water, and (3) whether the extratropical SAT trend pattern has become increasingly aligned over time with the SAT pattern associated with the anomalously warm western tropical Pacific water.

The reanalysis data and methods used to address these questions are described in section 2, followed by a presentation of the results in section 3. The conclusions of the study are discussed in section 4.

2. Data and Methods

The data used in this study are taken from the European Center for Medium Range Weather Forecasting (ECWMF) reanalysis (ERA-interim; Dee et al., 2011) over the 1979 to 2017 time period, with a horizontal resolution of 2.5°. All variables examined in this study are averaged over the winter months of December–February (DJF), the season for which the Arctic SAT has experienced the strongest upward trend (e.g., Screen & Simmonds, 2010)

To test the hypothesis that La Niña-like tropical convection has contributed to the SAT trend pattern (Lee, 2012), we first calculate the trends of the DJF SAT, sea level pressure (SLP), and SST over all consecutive 20-year time periods between 1979 and 2017. In order to preclude the effect of El Niño/Southern Oscillation (ENSO), these trends are calculated after ENSO is removed by subtracting the linear fit between each variable and the Niño 3.4 index (https://www.esrl.noaa.gov/psd/data/correlation/nina34.data), which we first normalize. The pattern being subtracted is indicated in Figure 1a, which shows the SAT regression map for a one standard deviation anomaly in the Niño 3.4 index.

We then calculate an additional index (denoted P_{sst}) to quantify the zonal gradient of the tropical Pacific SST as a metric for the La Niña-like state, which includes an enhanced SST in the western tropical Pacific:

$$P_{sst} = P_{west} - P_{east} \quad (1)$$

where P_{west} and P_{east}, respectively, denote the area-weighted domain average SST in the western (30 S–30°N, 120–180°E) and eastern (30°S–30°N, 70–177.5°W) tropical Pacific. The selection of these particular domains is motivated by an analysis of data provided online by NOAA PSD (the National Ocean and Atmospheric Administration Physical Science Division; https://www.esrl.noaa.gov/psd/cgi-bin/data/getpage.pl). Positive values of the P_{sst} index are associated with La Niña-like tropical condition.

The SAT pattern fitted linearly to the P_{sst} index (for a one standard deviation anomaly in the P_{sst} index) is almost indistinguishable from that fitted to the Niño 3.4 index (Figures 1a and 1b). Therefore, although we used the Niño 3.4 index to remove the ENSO signal because it is a standard index for ENSO, if the P_{sst} index is used instead to remove the ENSO signal, the resulting trend patterns (see Figure S1 in the supporting information) are again almost indistinguishable from the trend patterns obtained after the ENSO signal is removed using the Niño 3.4 index (Figure 2).

The linearly fitted patterns shown in Figure 1 are obtained after all data is detrended. Specifically, the P_{sst} and Niño 3.4 indices are detrended and the detrended DJF SAT and SLP anomaly fields (where an anomaly is defined by subtracting the DJF time mean) are regressed onto them, resulting in the SAT patterns shown in Figure 1.

To determine whether the extratropical SAT trend pattern has become increasingly aligned over time the SAT regression pattern shown in Figure 1b, we correlate each of the 20-year SAT (ENSO removed) trend patterns from 1979 to 2017 with it. These pattern correlations are uncentered and area-weighted. The same procedure is applied to the SST trends: The 20-year SST (ENSO removed) trend patterns over the tropical Pacific (30°S–30°N, 120°E–70°W) are correlated with the regression of the detrended SST onto the detrended P_{sst} index in that same region.

The statistical significance of the trends (Figure 2) and regression coefficients (Figure 1) is evaluated with a two-sided permutation test (a Monte-Carlo resampling procedure; Wilks, 2011) with 1,000 random resamplings (without replacement) of the data. We find this method to be highly consistent with the Student's t test (not shown). However, because the Student's t test cannot be easily applied to the pattern correlations, which have a far fewer number of degrees of freedom than the number of grid points in the domains (e.g., Horel, 1985), we determine their significance by correlating each of the 1,000 randomly generated trend maps with the regression map (Figure 1b). In other words, we generate a distribution of pattern correlations for each 20-year time period using the randomly generated trend maps from that same time period.

3. Results

The SAT and SLP trend patterns are shown in Figure 2 for each consecutive 20-year time period between 1979 and 2017. A transition from a cold-Arctic-warm-continent trend pattern, in years of past, toward a

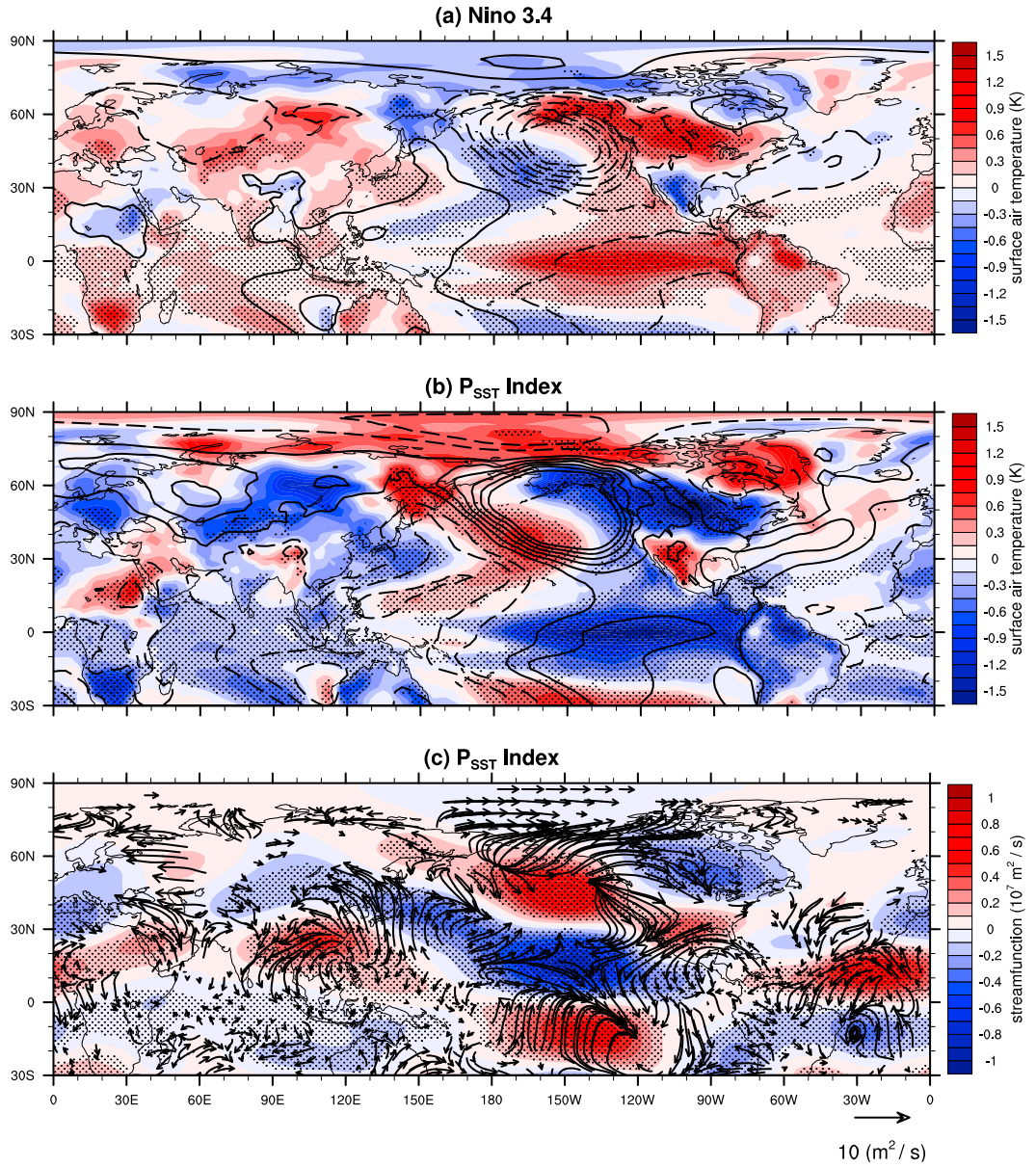

Figure 1. Detrended December–February (DJF) mean surface air temperature (colors) and sea level pressure (contours) regressed onto the detrended (a) Niño3.4 index and (b) P_{sst} index (see section 2). Negative contours are dashed. (c) The detrended DJF mean zonal-mean-removed stream function (colors) and wave activity flux (vectors) regressed onto the P_{sst} index. Small vectors with $p > 0.45$ are omitted for clarity. In all panels, stippling indicates statistical significance at $p < 0.10$ based on a two-sided permutation test (e.g., Wilks, 2011). Note that the wave flux is calculated daily before being averaged over each DJF season.

warm-Arctic-cold-continent trend pattern, in recent years, is evident, consistent with previous findings (e.g., Gong et al., 2017). This transition from a cold Arctic warm continent toward a warm Arctic cold continent SAT trend pattern is also accompanied by a consistent transition in the SLP trend pattern: The wind fields suggested by the SLP trend patterns can be used to infer SAT fields (Deser et al., 2016; Kutzbach, 1967; Namias, 1953; Teisserenc de Bort, 1883; Wallace & Gutzler, 1981) that are similar to the observed SAT trend patterns. Wherever the SLP trend implies southerly winds, warm air advection is to be expected and similarly for cold air advection where there are implied northerly winds. (It should be noted, however, that the zonal component of the wind can also contribute importantly to horizontal temperature advection (e.g., Thompson & Wallace, 2000)). For example, the warm Arctic cold continent SAT trend pattern for the

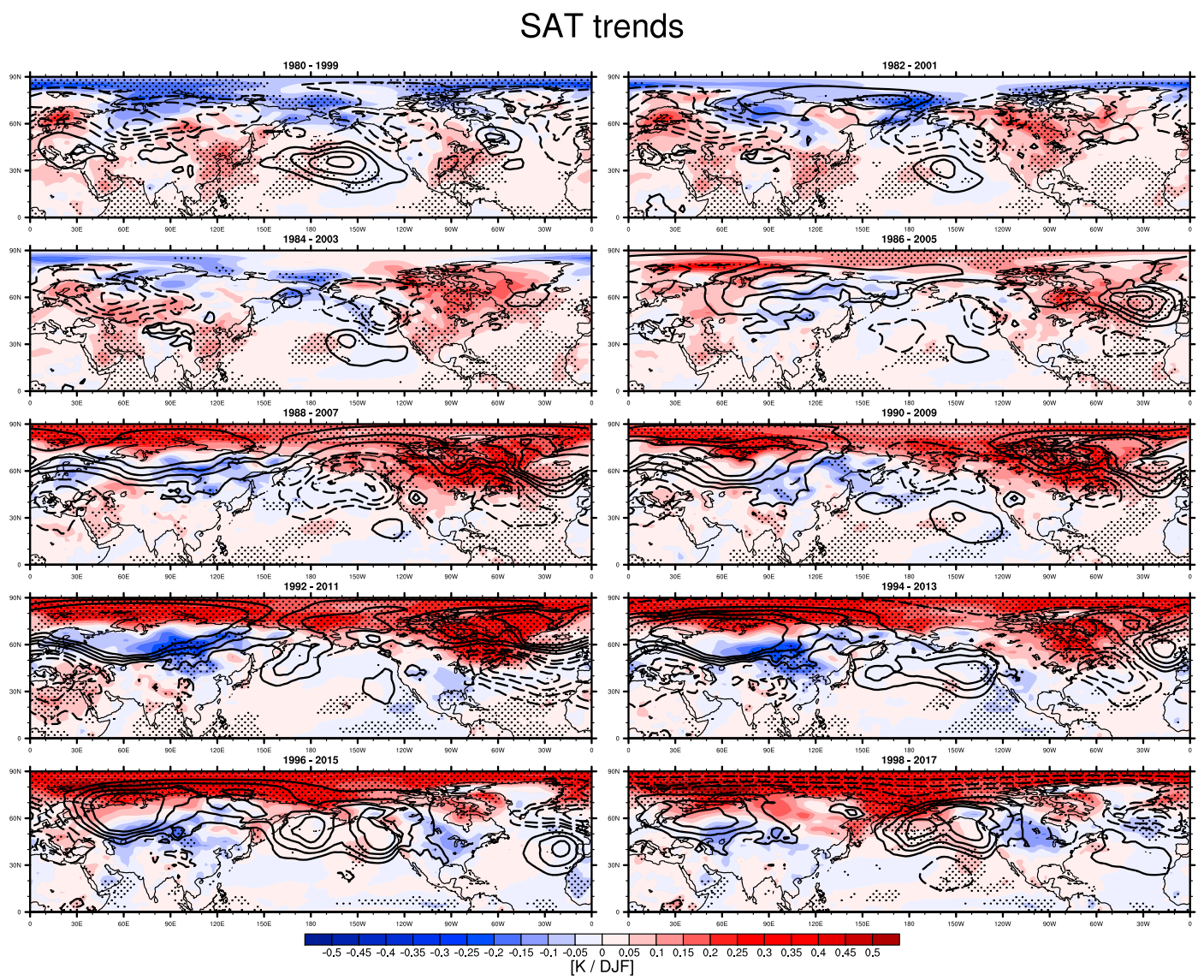

Figure 2. The December–February surface air temperature (colors) and sea level pressure (contours) trends over 20-year time periods (indicated by the titles) between 1979 and 2017 after subtracting the linear fit with the Niño 3.4 index. Negative contours are dashed. Stippling indicates statistical significance of the temperature field at $p < 0.10$ based on a two-sided permutation test (e.g., Wilks, 2011).

1992–2011 time period is characterized by a high-pressure trend pattern over Siberia and a negative NAO-like trend pattern over the North Atlantic that suggests warm air advection over the Arctic, where a warming trend is observed, and cold air advection over the continents, where a cooling trend is observed. This negative-NAO like trend pattern observed over the 1992–2011 time period disappears by the 1996–2015 time period and onward, consistent with a substantial weakening of the warming trend over the Baffin Bay region, where cold air advection is to be expected, and a slightly negative temperature trend over northwest Africa (also due to cold air advection).

Many of the trend patterns shown in Figure 2 resemble the pattern shown in Figure 1b, that is the regression of the detrended SAT and SLP anomalies onto the detrended P_{sst} index. This suggests that we can better understand the trends in Figure 2 by first considering the extratropical response to ENSO. Based on the regression patterns in Figure 1, the Arctic is expected to be anomalously warm and the continents anomalously cold during years when La Niña is active, consistent with findings of Lee (2012). Conversely, when El Niño is active, the Arctic is expected to be anomalously cold and the continents anomalously warm. The connection between La Niña and the warming observed over the Arctic is caused by poleward heat

and moisture fluxes associated with poleward propagating Rossby waves that constructively interfere with the climatological stationary wave (Goss et al., 2016) and are triggered by tropical convection (Lee, 2012). Given that the SAT trend patterns resemble El Niño before 1983 and La Niña thereafter (compare Figures 1, 2), the tropical convection trends for those respective time periods are expected to be characterized by spatial structures similar to El Niño and La Niña.

Although, in the extratropics, the 20-year SAT trend patterns beginning before 1983 are characterized by a pattern opposite to that shown in Figure 1b, those SAT trend patterns beginning after 1984 are characterized by a pattern similar to that shown in Figure 1b. Because ENSO (Figure 1a) was removed from the SAT prior to the computations of the trends shown in Figure 2 (see section 2), the transition toward this more La Niña-like extratropical SAT trend pattern cannot be a result of an increase in the frequency of occurrence of La Niña events. Rather, this transition toward a more La Niña-like SAT trend pattern seems to be associated with a long-term decadal timescale warming over the western tropical Pacific. To illustrate this point, the partial zonal mean tropical Pacific SST over the western and eastern domains (used to calculate the P_{sst} index) is shown as a function of time in Figures 3a and 3b, respectively. It is evident that the western tropical Pacific has undergone a long-term decadal timescale warming, whereas the eastern tropical Pacific has undergone multiple 1- to 3-year periods of warmer or colder than average SSTs. In accordance with the warming over the western tropical Pacific, Figure 3 also shows the rapid warming observed over the Arctic over the last 2 to 3 decades.

The pattern correlation (Figure 4) between each of the 20-year SAT trend maps (Figure 2) and the P_{sst} regression map (Figure 1b) quantifies the observation that the SAT trend is transitioning toward a more La Niña-like pattern. Specifically, poleward of 60°N, the correlations between the SAT trend patterns and P_{sst} regression map pattern has gradually grown from negative values, observed before 1983, toward positive values after 1983, that peak at a value of about 0.5 for the 1992-2011 time period. This transition toward positive pattern correlations is quite notable, given that the negative pattern correlations observed before 1983 lie outside of the 20th percentile, whereas those positive pattern correlations observed after 1984 lie oftentimes inside the 90th percentile.

In the midlatitudes, a similar, although more gradual, transition toward a more La Niña-like SAT trend pattern is apparent. For this region, negative pattern correlations are observed during those 20-year segments starting before 1991, whereas positive pattern correlations are observed thereafter. Similar to the Arctic, many of the positive pattern correlations in the midlatitudes are highly anomalous, residing in the 90th or 95th percentiles. However, in contrast with the Arctic, the timing of the positive pattern correlations is somewhat delayed. This finding that the Arctic transitions to a more La Niña like SAT trend pattern before the midlatitudes is consistent with Yoo et al. (2014), who showed that the Arctic SAT response to tropical convection is greater than the midlatitude SAT response to tropical convection. Perhaps synoptic timescale weather has contributed to the midlatitude SAT trend pattern more than it has contributed to the Arctic SAT trend, such that the response to tropical convection in the midlatitudes is weak and delayed relative to the response to tropical convection in the Arctic.

In recent decades, the tropical Pacific SST trend pattern has also become La Niña-like (Figure 4c). This transition of the SST trend toward a more La-Niña-like pattern is consistent with the observed transition toward a more La-Niña-like SAT trend pattern in the Arctic (Figure 4a) and extratropics (Figure 4b). Although the values of the pattern correlations for the tropical Pacific (Figure 4c) are not as significant as those in the Arctic (Figure 4a) or extratropics (Figure 4b), in all three sets of correlations, the values are positive and higher in the latter part of the time period. The strongest correlation between the tropical Pacific SST trend pattern (Figure S2) and corresponding regression map (Figure S3) lies within the 98th percentile and is observed during the time period ending in 2012 (Figure 4c).

It is important to note that any phenomenon associated with a warm Arctic will have pronounced positive pattern correlations with the SAT trend pattern over the Arctic in recent decades, regardless of any physical linkage to the Arctic SAT trend. However, in this case, the positive pattern correlations between Figure 2b and the trend maps of Figure 1 likely do reflect a physical linkage. The (zonal-mean-removed) regression of the stream function onto the P_{sst} index (Figure 1c) shows a Rossby wave train emanating from the tropical Pacific toward the Arctic and across the North American continent. This regression pattern resembles the stream function patterns that have been identified as being excited by tropical forcing

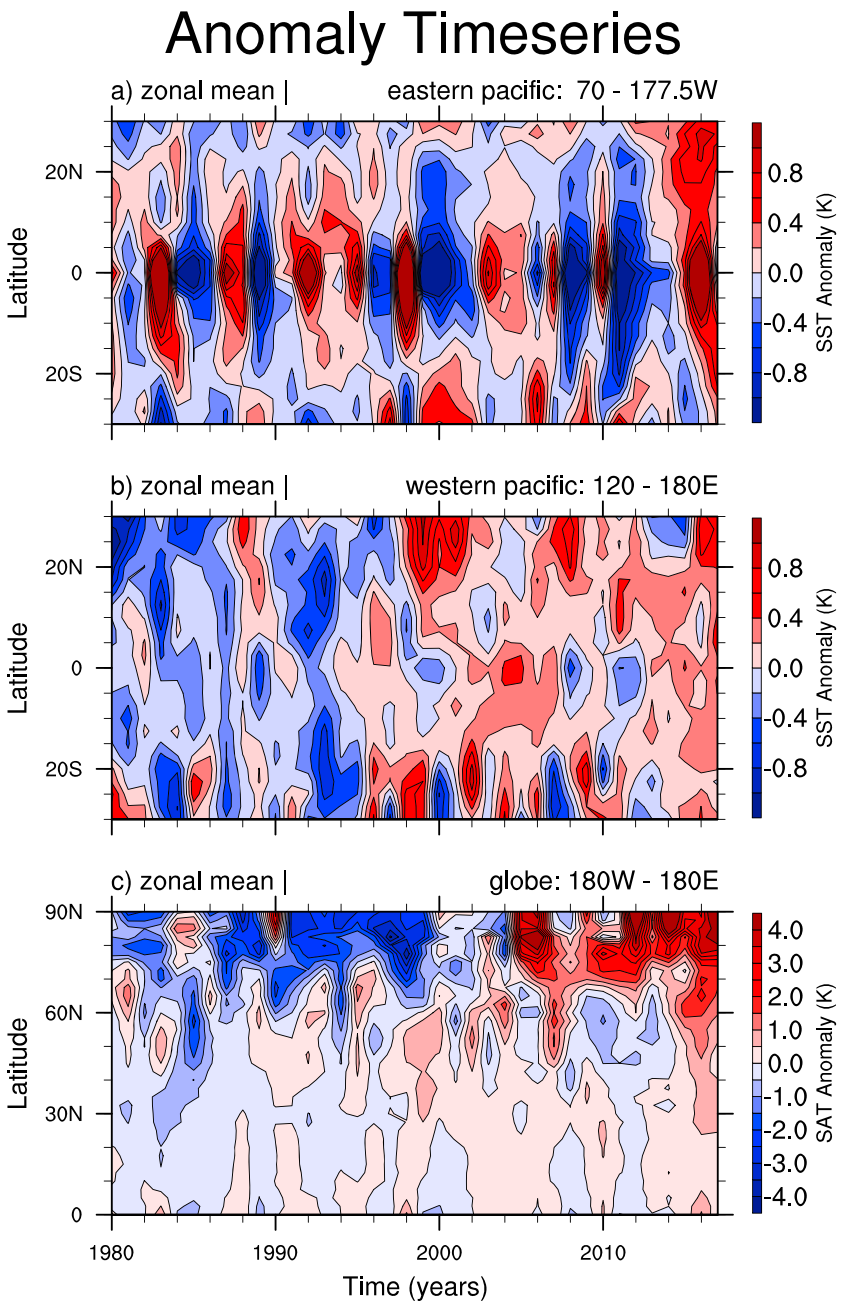

Figure 3. Wintertime (December–February) zonal mean of sea surface temperature over the (a) eastern and (b) western tropical Pacific. (c) The zonal mean time series of surface air temperature across all longitudes.

and driving Arctic warming (Baggett & Lee, 2015; Ding et al., 2014; Goss et al., 2016; Lee et al., 2011; Yoo et al., 2012).

The regression of wave activity flux (Takaya & Nakamura, 2001) onto the P_{sst} index also shows features consistent with TEAM. In the vicinity of the western Pacific warm pool, for example, the wave activity flux regressed onto the P_{sst} index has a pronounced poleward component (Figure 1c), similar to the wave activity flux trend of recent decades (Figure S4). These poleward wave activity fluxes likely originate from a Rossby wave source (Sardeshmukh & Hoskins, 1988) centered over western Pacific warm pool region. Although the wave activity fluxes entering the Arctic through the Bering Strait look to originate over the extratropics, they may also owe their existence to tropical convection over the western Pacific warm pool. The extratropical

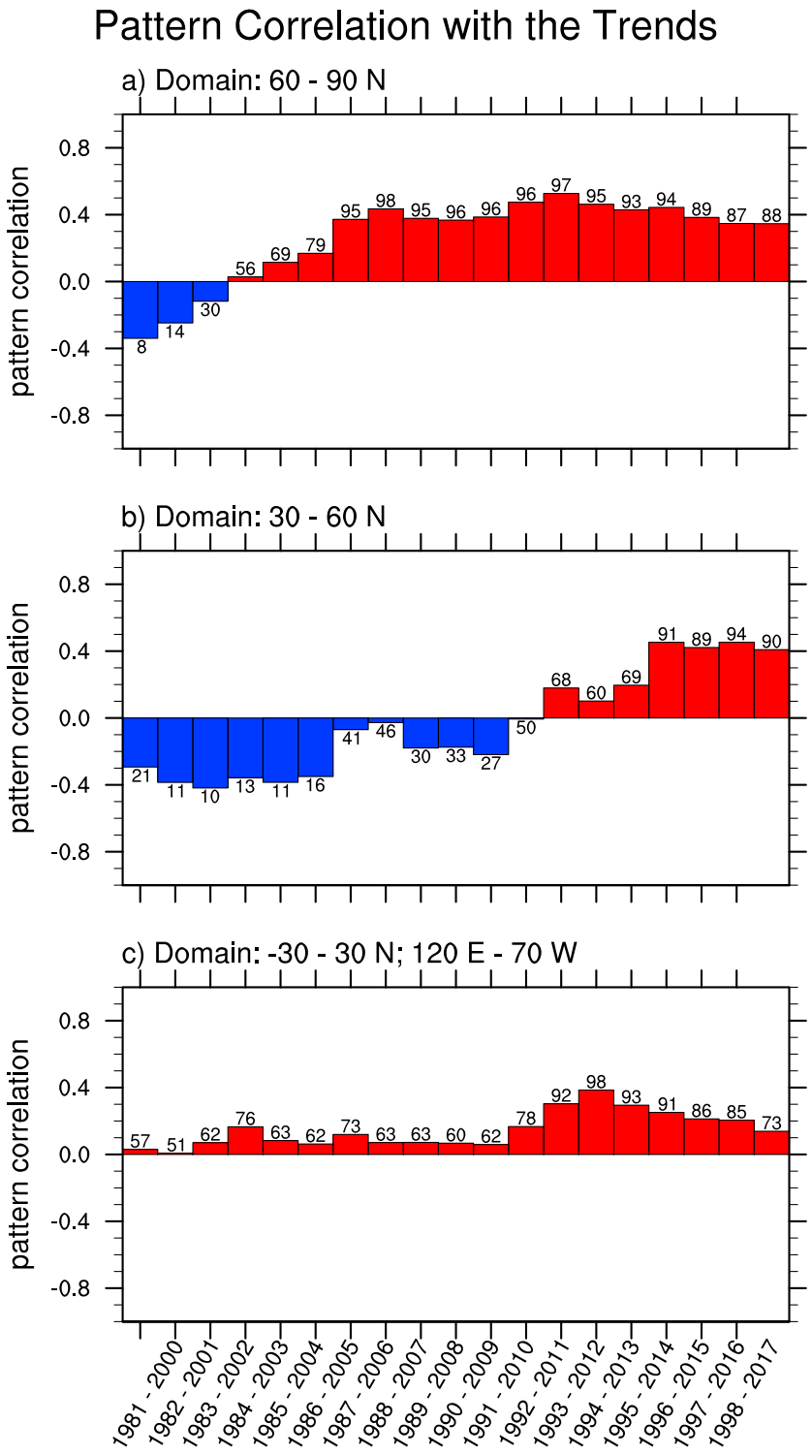

Figure 4. The pattern correlations between the 20-year surface air temperature trend patterns (Figure 1) over the (a) Arctic and (b) midlatitudes with the regression of the detrended December–February mean surface air temperature onto the detrended P_{sst} index (Figure 2b; see section 2). (c) The pattern correlations between the 20-year sea surface temperature trend patterns (Figure S1) with the regression of the detrended December–February mean sea surface temperature onto the detrended P_{sst} index (Figure S2). The number overlying or underlying any particular bar indicates the percentile that the pattern correlation represents based on the distribution formed by correlating each of the randomly generated trend maps (see section 2) of the corresponding time periods on the *x* axis with the appropriate regression map (Figure 2b or Figure S2).

diabatic heating that follows the wave trains forced by tropical convection can produce poleward propagating waves that subsequently warm the Arctic.

4. Summary and Conclusions

Over the last three decades, the wintertime Northern Hemisphere SAT trend has transitioned from a cold Arctic warm continent pattern toward a warm Arctic cold continent pattern, concurrent with an increase of the SST over the western tropical Pacific Ocean. Because this decadal timescale warming of the western tropical Pacific Ocean has occurred, while the SST trend over the eastern tropical Pacific Ocean has remained neutral, the east-west SST gradient over the tropical Pacific Ocean has increased. Several studies suggest that an increased east-west SST gradient can impart temperature changes in midlatitudes via the TEAM, which is characterized by poleward propagating Rossby waves that are triggered by La Niña-like tropical convection (Lee, 2012, 2014). This prompted an investigation into whether the TEAM has contributed to the transition of the SAT trend from a cold Arctic warm continent toward a warm Arctic cold continent pattern.

In contrast with the viewpoint that sea ice decline has driven the warm Arctic cold continent SAT trend pattern observed in recent decades (e.g., Nakamura et al., 2016; Sun et al., 2015; Zhang et al., 2018), in this study, we find that the extratropical response to La-Niña-like convection (i.e., the TEAM) has likely contributed to this warm Arctic cold continent SAT trend pattern. This conclusion follows from the regression of the detrended SAT field onto the detrended P_{sst} index (see section 2), which shows a warm Arctic cold continent pattern much like the SAT trend pattern observed in recent decades, consistent with (Lee, 2012, 2014). This conclusion is further supported by the result that the transition of the SAT trend from a cold Arctic warm continent toward a warm Arctic cold continent pattern is largely driven by horizontal temperature advection (as implied by the SLP trend pattern).

Because the linear fit between the SAT anomalies and the Niño 3.4 index is subtracted prior to the calculation of the SAT trends, the transition of the SAT trends toward a more La Niña-like pattern cannot be a result of the trend in the frequency of occurrence of La Niña events. Instead, the SAT trend pattern seems to be linked to a decadal timescale warming trend over the western tropical Pacific. This decadal timescale warming is unassociated with ENSO events and is therefore not likely a result of internal variability (e.g., Sun et al., 2016). Therefore, the contribution by the TEAM to the warm Arctic cold continent SAT trend pattern observed in recent decades may reflect a forced response, rather than internal variability.

Acknowledgments
The ERA-interim data used in this study can be downloaded from the ECMWF data server. We would like to thank Steven B. Feldstein for reviewing this article. We also thank an anonymous reviewer and Qinghua Ding for their helpful comments. This manuscript benefitted from helpful discussions with Mingyu Park and Dong Wan Kim. This study was supported by National Science Foundation grants OPP-1723832 and AGS-1822015.

References

Baggett, C., & Lee, S. (2015). Arctic warming induced by tropically forced tapping of available potential energy and the role of the planetary-scale waves. *Journal of the Atmospheric Sciences*, *72*(4), 1562–1568. https://doi.org/10.1175/jas-d-14-0334.1

Baggett, C., Lee, S., & Feldstein, S. (2016). An investigation of the presence of atmospheric rivers over the North Pacific during planetary-scale wave life cycles and their role in Arctic warming. *Journal of the Atmospheric Sciences*, *73*(11), 4329–4347. https://doi.org/10.1175/JAS-D-16-0033.1

Budyko, M. I. (1969). The effect of solar radiation variations on the climate of the Earthearth. *Tellus*, *21*(5), 611–619. https://doi.org/10.3402/tellusa.v21i5.10109

Chylek, P., Folland, C. K., Lesins, G., Dubey, M. K., & Wang, M. (2009). Arctic air temperature change amplification and the Atlantic Multidecadal Oscillation. *Geophysical Research Letters*, *36*, L14801. https://doi.org/10.1029/2009GL038777

Cohen, J., Screen, J. A., Furtado, J. C., Barlow, M., Whittleston, D., Coumou, D., et al. (2014). Recent Arctic amplification and extreme mid-latitude weather. *Nature Geoscience*, *7*(9), 627–637. https://doi.org/10.1038/ngeo2234

Cohen, J. L., Furtado, J. C., Barlow, M. A., Alexeev, V. A., & Cherry, J. E. (2012). Arctic warming, increasing snow cover and widespread boreal winter cooling. *Environmental Research Letters*, *7*(1), 014007. https://doi.org/10.1088/1748-9326/7/1/014007

Dee, D. P., Uppala, S. M., Simmons, A. J., Berrisford, P., Poli, P., Kobayashi, S., et al. (2011). The ERA-Interim reanalysis: Configuration and performance of the data assimilation system. *The Quarterly Journal of the Royal Meteorological Society*, *136*(653), 1972–1990. https://doi.org/10.1002/qj.722

Deser, C., Terray, L., & Phillips, A. S. (2016). Forced and internal components of winter air temperature trends over North America during the past 50 years: Mechanisms and implications. *Journal of Climate*, *29*(6), 2237–2258. https://doi.org/10.1175/jcli-d-15-0304.1

Deser, C., Tomas, R., Alexander, M., & Lawrence, D. (2010). The seasonal atmospheric response to projected Arctic sea ice loss in the late twenty-first century. *Journal of Climate*, *23*(2), 333–351. https://doi.org/10.1175/2009jcli3053.1

Ding, Q., Wallace, J. M., Battisti, D. S., Steig, E. J., Gallant, A. J. E., Kim, H.-J., & Geng, L. (2014). Tropical forcing of the recent rapid Arctic warming in northeastern Canada and Greenland. *Nature*, *509*(7499), 209–212. https://doi.org/10.1038/nature13260

Francis, J. A., & Vavrus, S. J. (2012). Evidence linking Arctic amplification to extreme weather in mid-latitudes. *Geophysical Research Letters*, *39*, L06801. https://doi.org/10.1029/2012GL051000

Garfinkel, C. I., Feldstein, S. B., Waugh, D. W., Yoo, C., & Lee, S. (2012). Observed connection between stratospheric sudden warmings and the Madden-Julian Oscillation. *Geophysiscal Research Letters*, *39*, L18807. https://doi.org/10.1029/2012GL053144

Garfinkel, C. I., Hartmann, D. L., & Sassi, F. (2010). Tropospheric precursors of anomalous Northern Hemisphere stratospheric polar vortices. *Journal of Climate*, *23*(12), 3282–3299. https://doi.org/10.1175/2010jcli3010.1

Gong, T., Feldstein, S. B., & Lee, S. (2017). The role of downward infrared radiation in the recent Arctic winter warming trend. *Journal of Climate*, *30*(13), 4937–4949. https://doi.org/10.1175/jcli-d-16-0180.1

Goss, M., Feldstein, S. B., & Lee, S. (2016). Stationary wave interference and its relation to tropical convection and Arctic warming. *Journal of Climate*, *29*(4), 1369–1389. https://doi.org/10.1175/jcli-d-15-0267.1

Horel, J. D. (1985). Persistence of the 500 mb height field during Northern Hemisphere winter. *Monthly Weather Review*, *113*(11), 2030–2042. https://doi.org/10.1175/1520-0493(1985)113<2030:potmhf>2.0.co;2

Kutzbach, J. E. (1967). Empirical eigenvectors of sea-level pressure, surface temperature and precipitation complexes over North America. *Journal of Applied Meteorology*, *6*(5), 791–802. https://doi.org/10.1175/1520-0450(1967)006<0791:eeoslp>2.0.co;2

Lee, S. (2012). Testing of the tropically excited Arctic warming mechanism (TEAM) with traditional El Niño and La Niña. *Journal of Climate*, *25*(12), 4015–4022. https://doi.org/10.1175/jcli-d-12-00055.1

Lee, S. (2014). A theory for polar amplification from a general circulation perspective. *Asia-Pacific Journal of Atmospheric Sciences*, *50*(1), 31–43. https://doi.org/10.1007/s13143-014-0024-7

Lee, S., Gong, T. T., Johnson, N. C., Feldstein, S. B., & Pollard, D. (2011). On the possible link between tropical convection and the Northern Hemisphere Arctic surface air temperature change between 1958-2001. *Journal of Climate*, *24*, 4350–4367. https://doi.org/10.1175/2011jcli4003.1

Lee, S., Woods, C., & Caballero, R. (2019). Relation between Arctic moisture flux and tropical temperature biases in CMIP5 simulations and its fingerprint in RCP8. 5 projections. *Geophysical Research Letters*, *46*, 1088–1096. https://doi.org/10.1029/2018GL080562

Nakamura, T., Yamazaki, K., Iwamoto, K., Honda, M., Miyoshi, Y., Ogawa, Y., et al. (2016). The stratospheric pathway for Arctic impacts on midlatitude climate. *Geophysical Research Letters*, *43*, 3494–3501. https://doi.org/10.1002/2016gl068330

Namias, J. (1953). The Relationship relationship of Mean mean Circulation circulation Patterns patterns to Weather weather and Climateclimate. In *Thirty-Day Forecasting: A Review of a Ten-Year Experiment*, *Meteorological Monographs* (Vol. 2, pp. 19–33). Boston, MA: American Meteorological Society. https://doi.org/10.1007/978-1-940033-07-5_1

Nishii, K., Nakamura, H., & Miyasaka, T. (2009). Modulations in the planetary wave field induced by upward-propagating Rossby wave packets prior to stratospheric sudden warming events: A case-study. *The Quarterly Journal of the Royal Meteorological Society*, *135*(638), 39–52. https://doi.org/10.1002/qj.359

Sardeshmukh, P. D., & Hoskins, B. J. (1988). The generation of global rotational flow by steady idealized tropical divergence. *Journal of the Atmospheric Sciences*, *45*(7), 1228–1251. https://doi.org/10.1175/1520-0469(1988)045<1228:tgogrf>2.0.co;2

Screen, J. A., & Francis, J. A. (2016). Contribution of sea-ice loss to Arctic amplification is regulated by Pacific Ocean decadal variability. *Nature Climate Change*, *6*(9), 856–860. https://doi.org/10.1038/nclimate3011

Screen, J. A., & Simmonds, I. (2010). The central role of diminishing sea ice in recent Arctic temperature amplification. *Nature*, *464*(7293), 1334. https://doi.org/10.1038/nature09051

Sellers, W. D. (1969). A global climate model based on the energy balance of the Earth earth-atmosphere system. *Journal of Applied Meteorology*, *8*(3), 392–400. https://doi.org/10.1063/1.5043957

Sorokina, S. A., Li, C., Wettstein, J. J., & Kvamstø, N. G. (2016). Observed atmospheric coupling between Barents Sea ice and the warm-Arctic cold-Siberian anomaly pattern. *Journal of Climate*, *29*(2), 495–511. https://doi.org/10.1175/jcli-d-15-0046.1

Sun, L., Deser, C., & Tomas, R. A. (2015). Mechanisms of stratospheric and tropospheric circulation response to projected Arctic sea ice loss. *Journal of Climate*, *28*, 7824–7845. https://doi.org/10.1175/jcli-d-15-0169.1

Sun, L., Perlwitz, J., & Hoerling, M. (2016). What caused the recent "Warm Arctic, Cold Continents" trend pattern in winter temperatures? *Geophysical Research Letters*, *43*, 5345–5352. https://doi.org/10.1002/2016gl069024

Takaya, K., & Nakamura, H. (2001). A formulation of a phase-independent wave-activity flux for stationary and migratory quasigeostrophic eddies on a zonally varying basic flow. *Journal of the Atmospheric Sciences*, *58*(6), 608–627. https://doi.org/10.1175/1520-0469(2001)058<0608:afoapi>2.0.co;2

Teisserenc de Bort, L. P. (1883). Etude sur l'hiver l'hiver de 1879–80 et recherches sur l'influence l'influence de la position des grands centres d'action d'action de l'atmosphère l'atmosphère dans les hivers anormaux. *Annales de la Societe Météorologique de France*, *31*, 70–79.

Thompson, D. W., & Wallace, J. M. (2000). Annular modes in the extratropical circulation. Part I: Month-to-month variability. *Journal of Climate*, *13*(5), 1000–1016. https://doi.org/10.1175/1520-0442(2000)013<1000:amitec>2.0.co;2

Trenberth, K. E., Fasullo, J. T., Branstator, G., & Phillips, A. S. (2014). Seasonal aspects of the recent pause in surface warming. *Nature Climate Change*, *4*(10), 911–916. https://doi.org/10.1038/nclimate2341

Wallace, J. M., & Gutzler, D. S. (1981). Teleconnections in the geopotential height field during the Northern Hemisphere winter. *Monthly Weather Review*, *109*(4), 784–812. https://doi.org/10.1175/1520-0493(1981)109<0784:titghf>2.0.co;2

Wilks, D. S. (2011). Frequentist Statistical Inference. In R. Dmowska, D. Hartmann, & H. T. Rossby (Eds.), *Statistical Methods in the Atmospheric Sciences*, *International Geophysics Series* (3rd ed., Vol. 100, pp. 133–186). Waltham, MA: Academic Press. https://doi.org/10.1016/b978-0-12-385022-5.00005-1

Woods, C., & Caballero, R. (2016). The role of moist intrusions in winter Arctic warming and sea ice decline. *Journal of Climate*, *29*(12), 4473–4485. https://doi.org/10.1175/jcli-d-15-0773.1

Woods, C., Caballero, R., & Svensson, G. (2017). Representation of Arctic moist intrusions in CMIP5 models and implications for winter climate biases. *Journal of Climate*, *30*(11), 4084–4102. https://doi.org/10.1175/jcli-d-16-0710.1

Yoo, C., Feldstein, S. B., & Lee, S. (2014). The prominence of a tropical convective signal in the wintertime Arctic temperature. *Atmospheric Science Letters*, *15*(1), 7–12. https://doi.org/10.1002/asl2.455

Yoo, C., Lee, S., & Feldstein, S. (2012). Arctic response to an MJO-like tropical heating in an idealized GCM. *Journal of the Atmospheric Sciences*, *69*, 2379–2393. https://doi.org/10.1175/jas-d-11-0261.1

Zhang, P., Wu, Y., Simpson, I. R., Smith, K. L., Zhang, X., De, B., & Callaghan, P. (2018). A stratospheric pathway linking a colder Siberia to Barents-Kara Sea sea ice loss. *Science Advances*, *4*(7), eaat6025. https://doi.org/10.1126/sciadv.aat6025